**SciencePG**
Science Publishing Group

# Kinetics and Thermodynamic Studies for Rhodamine B Dye Removal onto Graphene Oxide Nanosheets in Simulated Wastewater

**Owolabi Mutolib Bankole[*], Oluwatoba Emmanuel Oyeneyin, Segun Esan Olaseni, Olaniran Kolawole Akeremale, Pelumi Adanigbo**

Hydrochemistry Laboratory, Department of Chemical Sciences, Adekunle Ajasin University, Akungba, Nigeria

**Email address:**
bankolemutolib@yahoo.com (O. M. Bankole)
[*]Corresponding author

**To cite this article:**
Owolabi Mutolib Bankole, Oluwatoba Emmanuel Oyeneyin, Segun Esan Olaseni, Olaniran Kolawole Akeremale, Pelumi Adanigbo. Kinetics and Thermodynamic Studies for Rhodamine B Dye Removal onto Graphene Oxide Nanosheets in Simulated Wastewater. *American Journal of Applied Chemistry*. Vol. 7, No. 1, 2019, pp. 10-24. doi: 10.11648/j.ajac.20190701.12

**Abstract:** This report describes for the first time the kinetics, thermodynamic and optimized conditions for maximum removal of Rhodamine B in aqueous solution onto nanosheets of graphene oxides. Results from the GONS characterizations: UV, TEM, FTIR, EDX and XRD, revealed successful introduction of oxygen functionalities on the pristine graphite lattices. Adsorptive behaviour of RhB dye onto GONS under different experimental conditions such as pH, initial concentrations, adsorbent dosage, temperature, and contact time, were fully discussed in this work. The study showed that ≈93% of RhB was removed from simulated wastewater at; sorbent mass of 16.67mg; pH of 6.5; temperature of 298$K$; contact time of 60min; and concentrations ranging from 2.5 to 30mg/L. Experimental data tested against results of the kinetics and adsorption isotherm models, revealed that the sorption of RhB were best described by pseudo-second order and Freundlich models, respectively. Regeneration of the spent adsorbent was investigated using water, methanol and methanol/acetic acid (9:1) solution, as desorbing eluents. Methanol solution of acetic acid was observed to remove up to 94% of adsorbed RhB from GO surface compared to water (71.36%), and methanol (45.52%). The ease at which RhB was eluted from RhB-loaded GO using methanol/acetic acid (9:1), methanol and water shows that the adsorption mechanism is best described by physisorption.

**Keywords:** Graphene Oxide, Rhodamine B Dye, Adsorption, Kinetics, Thermodynamics, Wastewater

## 1. Introduction

Rhodamine B, RhB, is a synthetic cationic dye which belonged to the family of xanthenes [1]. It has gained promising applications in diverse areas such as molecular imaging [2, 3], laser dyes [4, 5], pigments, fluorescence standards, and as fluorescent probes [6, 7], due to its excellent photophysical and photostability properties [1]. Furthermore, RhB is regarded as essential raw material in textile, tannery, and paper mill industries [8, 9]. Increasing demand for the use of RhB in the aforementioned industries has increased their release into aquatic environment directly without treatment, thereby posing great dangers to both human and aquatic lives. Also, presence of RhB dye in water even at low concentration could reduce the quality of water thereby making it unfit for drinking and agricultural activities. Because of the potential carcinogenicity and neurotoxicity of RhB dye [10], their removal from effluents using low-cost and eco-friendly material is of great importance.

Popular among the methods that have been reported for the removal of organic dyes in wastewater are chemical oxidation, photochemical, ion exchange, irradiation, ozonation, and electrochemical destruction [11-17]. These methods however suffer from drawbacks such as the use of toxic and expensive chemicals, laborious reaction times, generation of hazardous by-products, and expensive equipment among others. These shortcomings can be overcome or avoided by using physical adsorption methods. Adsorption processes have been reported as an efficient, eco-

friendly and low-cost technique for the treatment of dye wastewater. This separation process is also efficient in the recovery of spent adsorbents using appropriate desorbing solvents [18].

Graphite, a weakly bonded stack of graphene layers has attracted great attention as adsorbent to remove pollutants from water due to its unique physicochemical properties [19-22]. One method of improving adsorption capacity of graphite is through oxidative treatment of pristine graphite using strong acids and oxidants, followed by exfoliation and dispersion of oxidized (graphite oxide) layers of graphene sheets in water [23]. The large surface area and the plurality of oxygen functionalities on graphene oxide could play significant roles in the abstraction of oppositely charged organic dyes from aqueous solution [24]. Comparative adsorption studies on the removal of cationic dyes, methylene blue and malachite green, by Bradder et al. [25], showed that graphene oxide has higher adsorption capacity, and shorter equilibration time compared to pristine graphite. Enhanced adsorption activity of layered graphite oxide was due to the electrostatic interactions between the negatively charged species of layered graphite oxide, and the cationic dyes [25]. Similar adsorption mechanism was also reported for the adsorption of methyl green using graphene oxide nanosheets [26]. Thus, exfoliated graphene oxide nanosheets are regarded as promising adsorbents for cationic dyes in solution.

The present work describes for the first time optimum conditions for maximum removal of cationic dye, Rhodamine B (RhB), using dispersed graphene oxide nanosheets in water. It is noteworthy to mention that removal of RhB using exfoliated graphene oxide has been reported before by Ramesha et al. [27]. Surprisingly, they observed that the percentage removal efficiency of RhB onto EGO decreases with increase in pH, hence EGO showed poor adsorption behavior for RhB amongst the studied cationic dyes [27]. This observation is in sharp contrast to the recent studies on the adsorption of RhB onto different anionic adsorbents [28-31]. Previous studies have shown that adsorption behavior and/or performance of GO are dictated by its method of preparation [32]. Herein, GONs was facilely prepared under ambient conditions, without intercalating the pristine graphite with bisulfate ions ($H_2SO_4/HNO_3$) at high temperature ($\approx 800°C$), as reported by Ramesha et al [27]. To the best of our knowledge, optimized kinetics and thermodynamic studies for maximum RhB removal onto graphene oxide nanosheets has not been reported before. Our aim, therefore, is to investigate the removal of cationic dye, RhB, onto nanosheets of graphene oxide with emphasis on the kinetics and thermodynamic study for its removal, and compare the performance of our as-synthesized GONS to other adsorbents that has been reported for RhB removal in aqueous solution. Optimized conditions for RhB described in this work include effects of temperature and its parameters, GONS dosage, pH, contact time and RhB concentrations. Also, regeneration of the spent adsorbent to verify the mechanism of adsorption is reported in this manuscript for the first time.

## 2. Materials and Methods

### 2.1. Materials

Graphite flakes, sulphuric acid (98%), potassium permanganate (99%), hydrogen peroxide (30% by vol.), hydrochloric acid, ethanol (99%) were supplied by Merck. Potassium nitrate ($KNO_3$, AR), sodium hydroxide (NaOH) and Rhodamine B (RhB, technical grade) were purchased from Sigma-Aldrich. All solvents were of analytical grades and used as received. Double distilled water was used throughout the experiments.

### 2.2. Preparation of Graphite Oxide (GO)

The graphene oxide was prepared by oxidation of pristine graphite flakes following modified Hummer's method [33, 34]. Typically, $KMnO_4$ (3 g) was slowly added to the slurry mixture of graphite flakes (1 g) and sulphuric acid (25 mL) placed in an ice bath to maintain temperature below 20°C. After addition of $KMnO_4$, the mixture was warmed up to 35 °C and maintained at the same temperature for 2 hr. Then 100 mL deionized water was slowly added to the reaction mixture, followed by addition of 10 mL (30 wt.%) of $H_2O_2$ solution until the color of the solution turned bright yellow. The mixture was watched and centrifuged repeatedly using 5% (by volume) hydrochloric acid solution, and distilled water to remove excess $KMnO_4$. The prepared graphite oxide was then dried under vacuum at 25°C for 24 hr.

### 2.3. Characterization of Adsorbent (GONS)

Absorption behavior of GONS adsorbent in aqueous solution was monitored using double beam (Shimadzu, UV-2550) spectrophotometer. Infra-red spectra of the adsorbent before and after experiments were recorded on a Thermo Fisher Scientific FTIR spectrophotometer, using pressed KBr pellets. Transmission electron microscope (TEM) image was recorded using a JEOL JEM-2010 electron microscope operating at 200 KV. The XRD spectrum was obtained with Bruker D8 ADVANCE diffractometer (Germany) using Cu Kα (1.5406 Å) radiation. EDX spectrum of GO was measured with a Si (Li) EDS detector (ThermoScientific) or an XFlash® SDD detector (Bruker), both having an active area of 10mm2. The pH of point of zero charge ($pH_{PZC}$) which measures the point at which the adsorbent is neutral was determined for the GONS using previously reported solid addition methods [35, 36].

### 2.4. Preparation of Adsorbate

Stock solution of the adsorbate was prepared by dissolving 10 mg of Rhodamine B (RhB) into 100 mL double distilled water to make concentration of 100 mg/L. Standard calibration curve between known concentrations (1 to 10 mg/L) of dye solutions was plotted against their respective absorbance at wavelength of 554 nm ($\lambda_{max}$ of RhB), using UV-Vis (model: Shimadzu, UV-2550) spectrophotometer. Unless noted otherwise, initial and residual concentrations of the dye solutions for the adsorption experiments were obtained from the standard calibration curve.

## 2.5. Batch Adsorption Experiments

Prior to the adsorption experiments, adsorbent for the dye removal was prepared by dispersing 0.2 g of graphite oxide in 300 mL double distilled water, and exfoliated into graphene oxide nanosheets (GONS) by sonication for 2 h. 25 mL of GONS solution (concentration: 0.67 mg/L) was added to 100 mL of different initial concentrations (2.5–30 mg/L) of RhB solution in a beaker of 250 mL capacity. The mixtures were agitated on a water-bath shaker (SHA-B, China) at fixed temperature of 25 °C, and optimum pH of 6.5 for a predetermined duration of 60 min. At the equilibration time of 60 min, the solutions were centrifuged at 10,000 rpm for 20 min, and the residual concentrations of RhB in the filtrates were analyzed spectrophotometrically at 554 nm. Equilibrium adsorption data were analyzed using the adsorption models listed in Table 1. Amount of RhB adsorbed ($q_e$ in mg/mg or mg/g) onto GONS, and the adsorption efficiency of the dye at equilibrium were estimated using Eqns. 1, [37] and 2, respectively.

$$q_e = \frac{C_0 V_{RhB} - C_e(V_{RhB} + V_{GONS})}{C_{GONS} V_{GONS}} \quad (1)$$

$$\% \text{ adsorbed} = \frac{(C_0 - C_e)}{C_0} \times 100 \quad (2)$$

where $C_0$ and $C_e$ (in mg/mL) are the initial and final concentrations of dye solution, $V_{RhB}$ and $V_{GONS}$ (mL) are respectively the volumes of RhB and GONS solution. $C_{GONS}$ (0.67 mg/mL) is the concentration of GONS solution.

Temperature-concentration adsorption profiles were studied by shaken 25 mL of GONS with 100 mL of RhB solution (30 mg/L) at an agitation speed of 120 rpm, and at different temperatures (25 °C, 35 °C, 45 °C and 55 °C). GONS dosage effects were investigated by agitating appropriate dosage of the GONS (5 mL to 25 mL) with 100 mL (30 mg/L) RhB solution at room temperature. In each case, samples were withdrawn at the equilibration time of 60 min, or at different contact time (0 min, 1 min, 3 min, 5 min, 10 min, 20 min, 30 min, 40 min, 50 min and 60 min for adsorption kinetics studies). Kinetics models listed in Table 2 were used to investigate the adsorption of RhB onto GONS. pH-concentration adsorption dependence of RhB onto GONS was also investigated by adjusting the pH of RhB (30 mg/L) solution from 2 to 10, using appropriate amount of (0.1 mol/L) NaOH or HCl solutions. Adsorption studies were carried out by agitating 100 mL of adjusted RhB solutions to 25 mL of GONS for 60 min, and at room temperature. The residual RhB concentrations were determined from the calibration curve [38] at absorbance maxima, $\lambda_{max}$ = 554 nm.

*Table 1. Adsorption isotherm models for RhB adsorption onto GONS.*

| Isotherms | Linear form | Plot[a] | Parameters[b] | Ref. |
|---|---|---|---|---|
| Langmuir | $\frac{1}{q_e} = \frac{1}{q_o} + \frac{1}{k_a q_o c_e}$ | $\frac{1}{q_e}$ vs $\frac{1}{c_e}$ | $k_a, q_o$ | 39 |
| Freundlich | $\log q_e = \log K_f + \frac{1}{n}\log c_e$ | $\log q_e$ vs $\log c_e$ | $K_f, n$ | 40 |
| D-R | $\ln q_e = \ln q_{DR} - \beta\varepsilon^2$ | $\ln q_e$ vs $\varepsilon^2$ | $q_{DR}, \beta$ | 41 |
| Tempkin | $q_e = \frac{RT}{b_T}\ln A_T + (\frac{RT}{b_T})\ln c_e$ | $q_e$ vs $\ln c_e$ | $b_T, A_T$ | 42 |
| Harkins-Jura | $\frac{1}{q_e^2} = \frac{B_{HJ}}{A_{HJ}} - (\frac{1}{A_{HJ}})\log c_e$ | $\frac{1}{q_e^2}$ vs $\log c_e$ | $A_{HJ}, B_{HJ}$ | 43 |

a$q_e$, equilibrium adsorption capacity of adsorbent (mg/g); $c_e$, equilibrium concentration of RhB in solution (mg/dm$^3$) and $\varepsilon$, Polanyi potential; b$q_o$, maximum monolayer capacity (mg/g); $k_a$, Langmuir isotherm constant (dm$^3$mg$^{-1}$); $K_f$, Freundlich isotherm constant (mg/g); $q_{DR}$, Dubinin-Radushkevich maximum adsorption capacity of RhB (mmol/g); n, adsorption intensity; $\beta$, Dubinin–Radushkevich isotherm constant (mol$^2$ kJ$^{-2}$); $b_T$, Tempkin isotherm constant; $A_T$, Tempkin isotherm equilibrium binding constant (dm$^3$g$^{-1}$); $A_{HJ}$, Harkins − Jura isotherm constant (mg/g)(mg/L)$^n$; $B_{HJ}$, Harkins-Jura adsorption intensity (L/mg).

*Table 2. Kinetics models for RhB adsorption onto GONS.*

| Model | Linear form | Plot[a] | Parameters[b] | Ref. |
|---|---|---|---|---|
| Pseudo-first order | $\ln(q_{e1} - q_t) = \ln q_{e1} - k_1 t$ | $\ln(q_{e1} - q_t)$ vs $t$ | $q_{e1}, k_1$ | 44-46 |
| Pseudo-second order | $\frac{t}{q_t} = \frac{1}{k_2 q_{e2}^2} + \frac{1}{q_{e2}}t$ | $\frac{t}{q_t}$ vs $t$ | $q_{e2}, k_2$ | 44-47 |
| Simple Elovich | $q_t = A + B\ln t$ | $q_t$ vs $t$ | $A, B$ | 48,49 |

a$q_e$, quantity of RhB adsorbed at equilibrium (mg/g) and $q_t$, quantity of RhB adsorbed at time $t$ (mg/g). b$k_1$, pseudo-first order rate constant (min$^{-1}$); $k_2$, pseudo-second order rate constant (g mg$^{-1}$ min$^{-1}$); $A$, adsorption rate constant (mg/g min); $B$, desorption rate constant (g/mg).

## 2.6. Data and Error Analysis

The results of the kinetics and sorption models were tested against the experimental data using linear coefficient of determination, $r^2$ , standard deviation, SD, standard uncertainty, $u$, and the nonlinear chi-square statistical test, $\chi^2$. The best fit between the kinetic (or isotherm) models to the experimental data gives smallest value of $\chi^2$, and vice versa. Mathematical representative of chi-square test is shown in Eqn. 3;

$$\chi^2 = \frac{\Sigma(q_{e,exp} - q_e)^2}{q_e} \quad (3)$$

where $q_{e,exp}$ is the experimental RhB adsorbed at equilibrium (mg/g) and $q_e$ as shown in Eqn. 1 above.

Also, mathematical representatives for standard deviation and standard uncertainty of errors are shown in Eqns. 4 and 5, respectively;

$$SD = \sqrt{\frac{q_{e,exp} - q_e}{n-2}} \quad (4)$$

$$u = \frac{SD}{\sqrt{n}} \quad (5)$$

where n is the number of data points in the set.

## 2.7. Desorption Studies

Regeneration studies on the spent adsorbent were investigated to determine possible reusability of the adsorbent after batch adsorption experiments. Desorption studies also give insight into mode of sorption process of RhB onto GONS. RhB was first loaded onto GONS by shaken aqueous solution of GONS (25 mL, concentration: 0.67 mg/L) with 100 mL of RhB solution (30 mg/L), under the same experimental conditions conducted for batch adsorption experiments. The RhB-adsorbent solution was centrifuged and the residual RhB concentration in the filtrates were analyzed spectrophotometrically at 554 nm. The RhB-loaded adsorbent was then dried under vacuum at 25℃ for 24 hr. Desorption of RhB from GONS surface was investigated by agitating pre-weighed RhB-loaded adsorbent with 100 mL each of desorbing eluents: water, methanol and methanol/acetic acid (9:1), for 1 h and at room temperature. The concentration of desorbed RhB was spectrophotometrically determined at $\lambda_{max}$ 554 nm. Efficiency of the desorbing eluents to regenerate the spent adsorbent can be determined by comparing amount of RhB in RhB-loaded adsorbent, to the amount of RhB desorbed from the adsorbent.

# 3. Results and Characterizations

## 3.1. Characterizations of Adsorbent

Modified Hummer's method was used to prepare graphite oxide using oxidative treatment of pristine graphite flakes in the presence of sulphuric acid and potassium per manganate. The oxidative treatment of the slurry mixture was quenched on addition of hydrogen peroxide. The obtained graphite oxide was homogenized by ultrasonic sonication to form stable and well dispersed exfoliated graphene oxide nanosheets (GONS) in water, Figure 1A (inset). Figure 1A, shows normalized electronic absorption spectrum of GO nanosheets layers recorded in water. The UV–Vis spectrum of the GONS revealed intense absorption peak at 210 nm, corresponding to the $\pi \to \pi^*$ transitions of aromatic $C - C$ bonds, and a shoulder around 311 nm, assigned to the $n \to \pi^*$ transitions of $C = O$ bonds in the graphene lattices. Elemental compositions of as-prepared graphene oxide were qualitatively verified using energy dispersive spectroscopy (EDS) in Figure 1B. The presence of elemental C and O confirmed the successful oxidation of natural graphite flakes to graphite oxide. Also, absence of other elements in the EDX spectra suggests that the prepared graphene oxide is free of other contaminants. The TEM micrograph in Figure 1C shows successful oxidation of the pristine graphite flakes evidenced from the numerous bends and wrinkles observed on the nanosheets of the GO. The numerous overlapping areas on the TEM image of the GONS shows that they are highly dispersed in water [50]; and easily exfoliated into several monolayers. The powder X-ray diffraction pattern of as-synthesized GONS (Figure 1D) material shows intense sharp peak at $2\theta = 10.02°$, which corresponds to 001 plane with d-spacing of 8.74 Å. The observed d-spacing value is higher than that of pristine graphite powder recorded at 3.56 Å [51], this indicates successful introduction of oxygen functionalities (epoxide, hydroxyl, carbonyl and carboxylate) on the pristine graphite lattices.
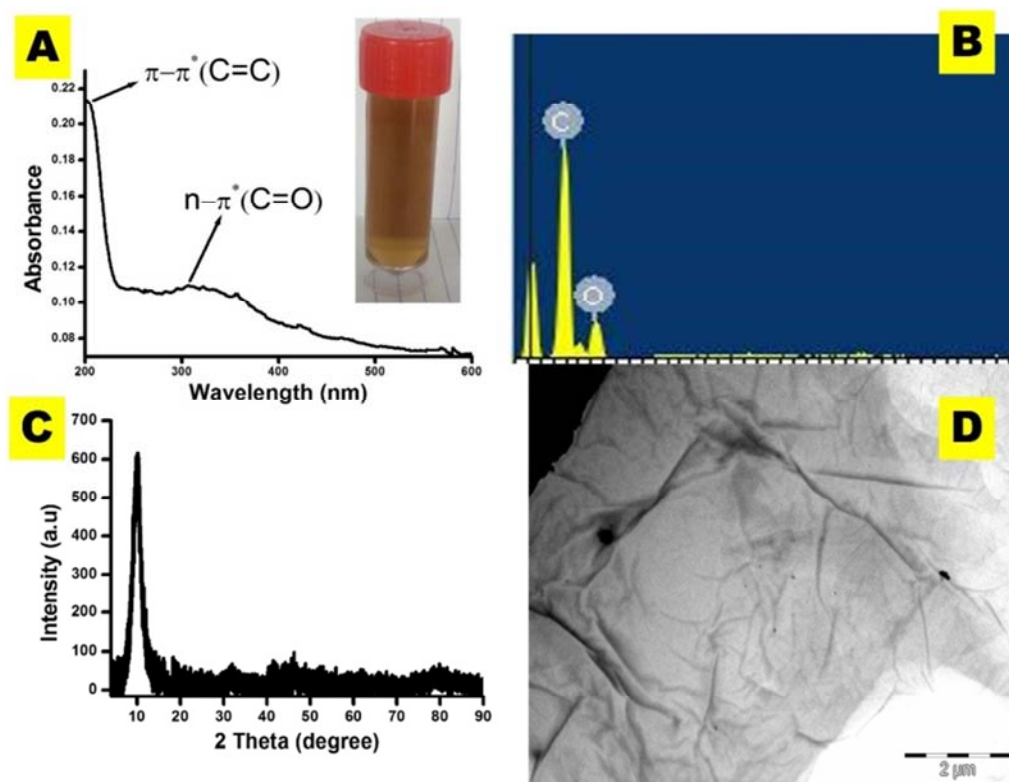


**Figure 1.** (A) Normalized UV–Vis absorption spectrum of GONS, exfoliated GO nanosheets in distilled water (inset), (B) EDX spectra of graphite oxide, (C) TEM image of GO nanosheets and (D) X-ray diffraction (XRD) patterns of GONS powder.

### 3.2. Batch Adsorption Experiments

The adsorption processes for the removal of RhB-contaminated waste water onto aqueous dispersion of GONS were investigated, using numbers of adsorption isotherms (listed in Table 1), and kinetics models (listed in Table 2). Factors such as change in pH, contact time, effect of temperature, GONS dosages; were also considered to determine optimum conditions which favoured maximum removal of RhB in water.

#### 3.2.1. pH-concentration Dependence Adsorption Profiles

Change in pH of dye solutions could affect the adsorptive behaviour of dyes to the sorbent surfaces, due to possible formation of different ionic species on the adsorbent surfaces, or change in the surface charge of the dye molecules [52]. Figure 2A shows the RhB dye uptake at various pH values from 2 - 10. It can be observed that the removal efficiency of RhB increased in a pH range from 2 and 10. The removal of RhB by GONS at ~ pH 2.01 was the minimum at 37.08% (or 40.35 mg/g), and a maximum of 88.85% (or 168.88 mg/g) removal was obtained at pH range of 6 – 8. A sharp decrease in the removal efficiency of RhB was observed at Ph > 8. The observed trends in RhB removal efficiency with increasing pH of the solution can be attributed to the change in the structure of RhB, and/or alteration to surface charge of the adsorbent under different conditions. Figure 2B shows the pH of point of zero charge ($pH_{PZC}$) of as-prepared GONS to be 2.12; this corresponds to the point at which the GONS was neutral. At $pH < pH_{PZC}$ , GONS exhibits cationic behaviour which account for poor removal of cationic RhB dye by GONS at $\approx$ pH 2.0, due to electrostatic repulsion between adsorbate and the adsorbent. At $pH > pH_{PZC}$, the surface of GONS becomes negatively charged with corresponding increase in RhB uptake by GONS, this is an indication of increasing electrostatic interaction between cationic RhB dye and anionic GONS with increasing pH from 2.0 to 8.0. However, as the basicity of the solution increases (i.e. pH > 8), monomers of RhB are electrostatically attracted to each other to form larger molecules (dimers) [53] that are too big to enter the pores of the GONS. The formation of larger quinonoid structure of RhB at pH > 8 led to drastic reduction in RhB uptake capacity ($q_e$) by GONS, as observed in Figure 2A. It could be inferred from the above results that change in the pH of RhB solution greatly influenced its adsorption capacity ($q_e$). Ramesha et al. [27] reported on the use of exfoliated graphene oxide (EGO) for the adsorption of various cationic and anionic dyes from aqueous solutions. However, percentage removal efficiency of RhB was found to decrease with increasing pH of the solution, therefore showing poor adsorption behaviour amongst the studied cationic dyes. The observed trends in their results are in sharp contrast to recent studies on the removal of RhB using different anionic adsorbents [28-31]. Here in, anionic GONS was facilely prepared at ambient conditions, and without intercalating the pristine graphite with bisulfate ions ($H_2SO_4/HNO_3$) at high temperature ($\approx$ 800 ℃), as reported by Ramesha et al [27]. Hence, enhanced adsorption behavior of our as-prepared GONS for RhB uptake compared to EGO could be attributed to the differences in their methods of preparation. Based on the adsorption capacity, the optimized pH value for maximum adsorption for RhB by GONS is 6.5, this is also in good agreement with previous studies on RhB as stated above [28-31].
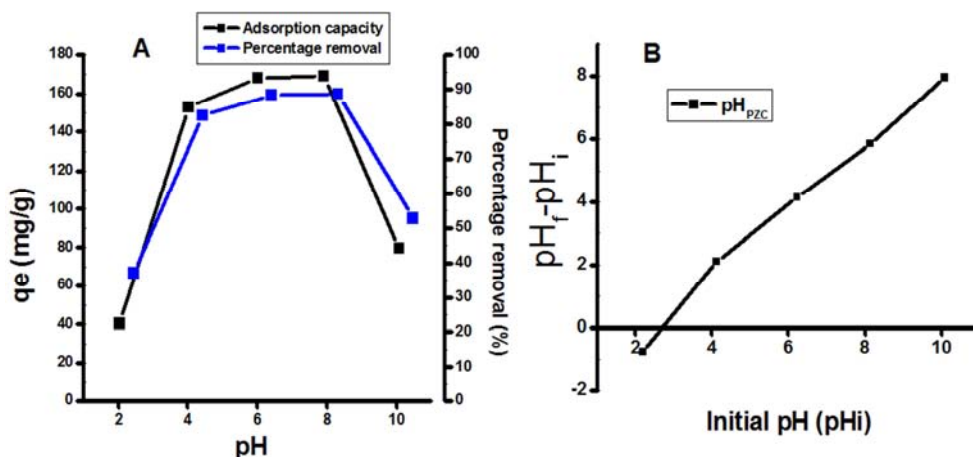


**Figure 2.** *(A) Variation of percentage removal efficiency and adsorption capacity of RhB ($C_o$ = 30 mg/L) on GONS as a function of pH, and (B) Plot of pH ($pH_f - pH_i$) against initial pH ($pH_i$) for determining the pH of point of zero charge ($pH_{PZC}$) of GONS.*

#### 3.2.2. Adsorbent Dose-concentration Dependence Study

Optimal adsorbent dosage of GONS for maximum uptake of RhB was investigated by contacting fixed concentration of RhB solution with varying concentrations of GONS dosage. Figure 3 shows the variation of RhB adsorbed (mg and/or %) plotted against different concentrations of GONS dosage (mL). The results revealed gradual reduction in the amount of RhB uptake from 599.49 to 165.64 mg/g with increase in adsorbent dosage from 5 (3.3 mg) to 25 mL (16.7 mg). This is attributed to possible overlapping or aggregation of dye molecules as a result of increased sorbent doses which could lead to reduction in the available active sorption sites for

sorbate removal [54, 55]; decrease in total surface area of adsorbent corresponds to increase in diffusional path length of the adsorbent [56]. RhB sorbed per unit mass of GONS was found to be at its maximum at the lowest adsorbent dosage of 3.3 mg in the work. The percentage removal of RhB was in reverse trend with increasing in the quantity of the adsorbent dosage, Figure 3. By increasing the quantity of adsorbent dosage of GONS, the total surface area and availability of more adsorption sites is increased, resulting in increasing percentage RhB removal from the solution.
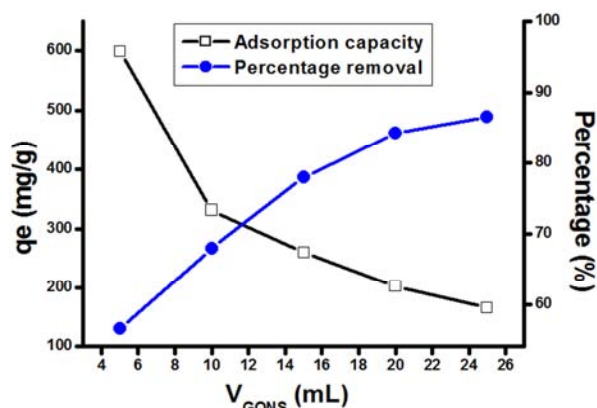


***Figure 3.*** *Effect of GONS dose on the adsorption of RhB. Conditions: Sorbent 3.3 - 16.67 mg in 25 mL of water, Sorbate 30 mg/L in 100 mL of water, 60 min equilibration time, pH 6.5, agitation speed 120 rpm, temperature 25℃].*

### 3.2.3. Effect of Contact Time and Adsorption Kinetics

Experimental investigation to determine the equilibration time for the abstraction of RhB from solution onto GONS was carried out at different time intervals, as shown in Figure 4A. It was observed that the amounts of RhB sorbed per unit mass of GONS decreased rapidly in the first 5 minutes for all the dye concentrations examined (30 mg/L as representative, Figure 4B), and no significant differences in the adsorption capacities were observed as the contact time increases to 60 min; an indication that equilibrium is reached within 5 min. The rapid uptake of RhB within the first 5 min can be attributed to the increased sorbent-sorbate interactions due to availability of large active sorption sites on the adsorbents, while insignificant differences in the adsorption capacities beyond 5 min, is due to saturation of adsorption sites on the GONS. The shorter the equilibrium time, the better the adsorbent. The equilibrium time of 5 min reported in this work is far lesser than those reported for carbon nanotube–cobalt ferrite nanocomposites (equilibrium time = 6 h) used for removal of RhB in aqueous solution [57], implying that the GONS has a better affinity for RhB compared to the composites of carbon nanotube–cobalt ferrites. Zhou et al. [37] have also demonstrated that GO is a better adsorbent than $Fe_3O_4$/GO composites, in terms of enhanced adsorption capacity of former, due to replacement of active adsorption sites on GO by $Fe_3O_4$ nanoparticles of $Fe_3O_4$/GO.
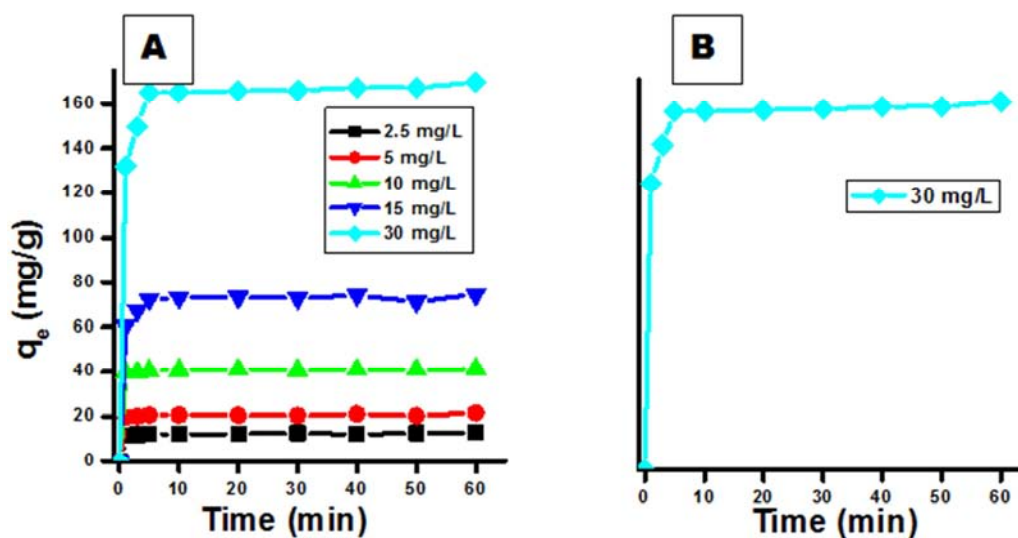


***Figure 4.*** *(A) Adsorption of RhB onto GONS as a function of contact time. Conditions: GONS 25 mg/L, RhB 2.5 to 30 mg/L, temperature* 25 ℃, *pH 6.5, agitation speed 120 rpm, sorbate volume 100 mL, (B) Representative contact time-concentration profile of RhB on GONS for 30 mg/L.*

Adsorption kinetics involved in the sorption of RhB onto GONS were studied using three different kinetic models; pseudo-first order [44-46], pseudo-second order [44-47], and Elovich models [48, 49]. Linearized form of the kinetics models and parameters are listed Table 2. The linear correlation coefficients, $r^2$, values for both pseudo-first order and elovich models were poor, and far lesser than 1.0 in all cases, Table 3, implying that the dynamics of sorption processes of RhB are not described by the above models.

However, $r^2$ values of pseudo-second order were close to unity for all the initial concentrations investigated, hence mechanism of the adsorption was attributed to the sorbate-sorbent bimolecular interactions between anionic charges on the surface of GONS, and cationic species of RhB in aqueous solution [58]. The calculated $q_e$ values obtained from pseudo-second order plots, Figure 5, were in good agreements with the values of $q_{e,exp}$ derived from the sorption experiments (Table 3). However, the disparities

between $q_e$ and $q_{e,exp}$ values for both pseudo-first-order kinetic and simple elovich models were very high. The value of $k_2$ ( g/(mg min) ) decreased with increase in the concentration of RhB. Initial sorption rate $h_o$ (g/(mg min)) which was obtained from linearized pseudo-second order model ( Eqn. 6 ), was in reverse trend to $k_2$. This is an indication that flow rate of the dye depends largely on the concentration of its ions in solution, and pseudo-second-rate constant ( $k_2$) is independent of particle diameter for chemically controlled sorption processes.

$$h_o = k_2 q_e^2 \qquad (6)$$

As stated above, results from the kinetics models were tested against sorption experimental data using SD, $u$, $\chi^2$, Eqns. 3, 4 and 5. It was observed that pseudo-second order has the lowest SD, $u$ and $\chi^2$ values amongst the tested models (Table 4), suggesting the process of sorption of RhB

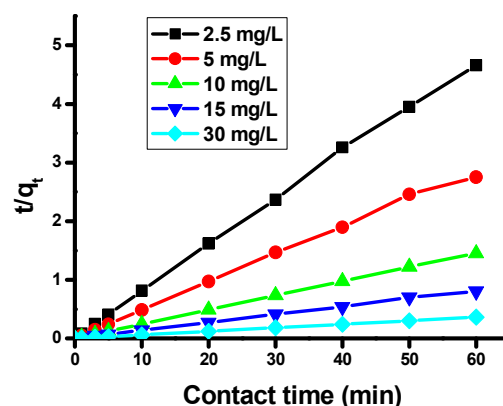was best described by pseudo-second order model.



**Figure 5.** *Pseudo-second-order kinetic plots for the removal of RhB by GONS as a function of contact time at different initial RhB concentrations (mg/L). [Conditions: sorbent mass 16.67 g in 25 mL; sorbate concentration 2.5 – 30 mg/L; sorbate volume, 100 mL; agitation speed, 120 rpm.].*

**Table 3.** Kinetics parameters for adsorption of RhB. Conditions: sorbent mass 16.67 mg in 25 mL; sorbate concentration 2.5 – 30 mg/L; sorbate volume, 100 mL; pH 6.5: agitation speed 120 rpm.

| Model | Parameters | Initial concentration (mg/L) | | | | |
|---|---|---|---|---|---|---|
| | | 2.49 | 4.79 | 9.87 | 15.09 | 29.85 |
| Experimental | $q_{e,exp}$/mg/g | 12.90 | 21.79 | 41.32 | 75.37 | 166.23 |
| Pseudo-first order | $q_{e1}$/mg/g | 1.20 | 1.40 | 2.46 | 5.47 | 4.81 |
| | $k_1$ /$min^{-1}$ | 0.05 | 0.01 | 0.05 | 0.02 | 0.03 |
| | $r^2$ | 0.649 | 0.100 | 0.356 | 0.278 | 0.216 |
| Pseudo-second order | $q_{e2}$/mg/g | 12.74 | 21.19 | 41.15 | 73.53 | 169.49 |
| | $k_2$/g/(mg min) | 0.27 | 0.25 | 0.15 | 0.09 | 0.02 |
| | $h_o$/g/(mg min) | 43.29 | 67.57 | 416. 7 | 500 | 625 |
| | $r^2$ | 0.999 | 0.999 | 0.999 | 0.999 | 1.000 |
| Simple Elovich | $A$/mg/(g min) | 11.66 | 12.99 | 26.08 | 42.33 | 93.62 |
| | $B$/g/mg $^{-1}$ | 0.26 | 2.40 | 4.54 | 9.36 | 21.71 |
| | $r^2$ | 0.795 | 0.327 | 0.304 | 0.409 | 0.430 |

**Table 4.** Error analysis for the kinetic data of the sorption of RhB on GONS.

| Model | Parameters | Initial concentration (mg/L) | | | | |
|---|---|---|---|---|---|---|
| | | 2.49 | 4.79 | 9.87 | 15.09 | 29.85 |
| Pseudo-first order | SD | 1.292 | 1.707 | 2.356 | 3.159 | 4.813 |
| | $\chi^2$ | 113.9 | 297.6 | 614.2 | 892.6 | 6547 |
| | $u$ | 0.431 | 0.569 | 0.785 | 1.053 | 1.605 |
| Pseudo-second order | SD | 0.142 | 0.276 | 0.145 | 0.480 | 0.638 |
| | $\chi^2$ | 0.002 | 0.017 | 0.001 | 0.046 | 0.063 |
| | $u$ | 0.045 | 0.087 | 0.046 | 0.152 | 0.202 |
| Simple Elovich | SD | 0.164 | 0.378 | 0.691 | 0.869 | 1.525 |
| | $\chi^2$ | 0.003 | 0.043 | 0.250 | 0.347 | 1.452 |
| | $u$ | 0.0546 | 0.126 | 0.230 | 0.290 | 0.508 |

### 3.2.4. Effect of Concentration and Adsorption Isotherms

To investigate the effect of initial sorbate concentrations, experiments were carried out at a fixed adsorbent volume of 25 mL (concentration: 0.67 mg/L), and at varying RhB concentrations of 2.49, 4.79, 9.87, 15.09 and 29.85 mg/L. The plot of sorbate adsorbed in mg/L versus initial concentrations (mg/L) of RhB (in Figure 6) shows that the RhB uptake by GONS increased in magnitude with positive slopes as the

initial concentrations of the dye increases. From the results presented in Table 5, it can be observed that the highest percentage RhB uptake was recorded at low adsorbate concentration. This is attributed to the availability of more active sites on the adsorbent. However, the active sorption sites on the adsorbent become increasingly saturated at higher concentrations of RhB, hence the observed relatively low percentage adsorption at higher RhB concentrations.

**Table 5.** Effect initial of concentration on adsorption of RhB on GONS. Conditions: sorbent mass 16.67 g in 25 mL; sorbate concentration 2.5 – 30 mg/L; sorbate volume, 100 mL; pH 6.5: agitation speed 120 rpm.

| Initial conc. (mg/L) | Initial abs | Final abs | Final conc. (mg/L) | Amount adsorbed (mg/L) | Percentage adsorbed (%) |
|---|---|---|---|---|---|
| 2.49 | 0.417 | 0.037 | 0.178 | 2.312 | 92.87 |
| 4.79 | 0.738 | 0.088 | 0.483 | 4.307 | 89.91 |

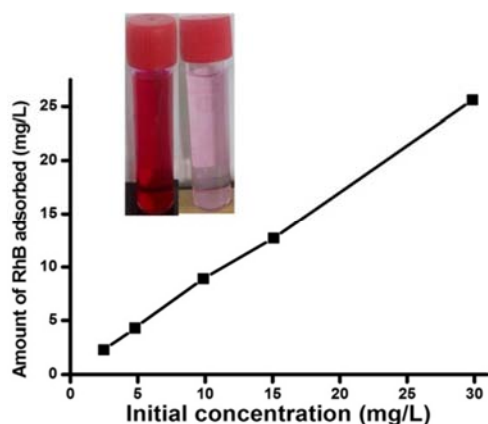| Initial conc. (mg/L) | Initial abs | Final abs | Final conc. (mg/L) | Amount adsorbed (mg/L) | Percentage adsorbed (%) |
|---|---|---|---|---|---|
| 9.87 | 1.401 | 0.166 | 0.960 | 8.910 | 90.27 |
| 15.09 | 2.683 | 0.403 | 2.397 | 12.693 | 84.12 |
| 29.85 | 5.684 | 0.702 | 4.216 | 25.634 | 85.88 |



**Figure 6.** *Adsorption of RhB onto GONS (16.67 mg) as a function of initial concentration (2.5 - 30 mg/L), RhB before and after adsorption study (inset).*

Adsorption isotherms models are used to describe the distribution and interactive behaviour of adsorbate partitioned between the solid (adsorbent) and liquid (aqueous solution) phase, as the adsorption process reaches equilibrium. Herein, Langmuir, Freundlich, Dubinin–Radushkevich (D-R), Tempkin and Harkins-Jura were adopted as representative isotherms models to describe the adsorption processes of RhB on GONS at equilibrium. The linearized forms of the tested models and their parameters are listed in Table 1. The magnitude of the parameters of the isotherm models which described the relationship between the sorption experimental and theoretical data are summarised in Table 6. The nature of surface binding and affinity of GONS to RhB were revealed from the isotherm curves shown in Figure 7A-E. From Table 6,

linear coefficient ($r^2$) values recorded for both Langmuir ($r^2 = 0.952$) and Freundlich ($r^2 = 0.998$) are closer to unity, hence sorption processes of RhB were more compatible with the Langmuir and Freundlich models than other tested models. However, Freundlich has the highest $r^2$ among the models tested, it is therefore adjudged as the isotherm model that best described the process of RhB sorption by GONS. The good agreement between the experimental data and Freundlich model suggests that the adsorption of RhB onto GONS followed multilayer adsorption processes, due to the heterogeneity nature of the sorbent surfaces, and/or possible interactions between the adsorbed Rhodamine B molecules. Previous study also established similar observations [27]. The magnitude of Freundlich isotherm constant ($K_f = 47.36$ mg/g) is higher in this work than for RhB by EGO ($K_f = 0.54$ mg/g) [27], and carbon nanotube–cobalt ferrite nanocomposites ($K_f = 1.120 - 31.03$ mg/g) [57], which suggests that GONS has relatively higher multilayer adsorption capacity for RhB than EGO and carbon nanotube–cobalt ferrite nanocomposites. The value of adsorption intensity, n, greater than 1 in this present work, indicates that Freundlich model is favourable for the sorption processes. Also, the value of Vermeulan criteria (Eqn. 7), expressed in terms of a dimensionless constant separation factor $R_L$ is less than unity [59, 60], suggesting that the adsorption of RhB on GONS is a favorable process.

$$R_L = 1(1 + k_a C_o) \qquad (7)$$

where $k_a$ and $C_o$ are Langmuir constant and initial concentration, respectively.
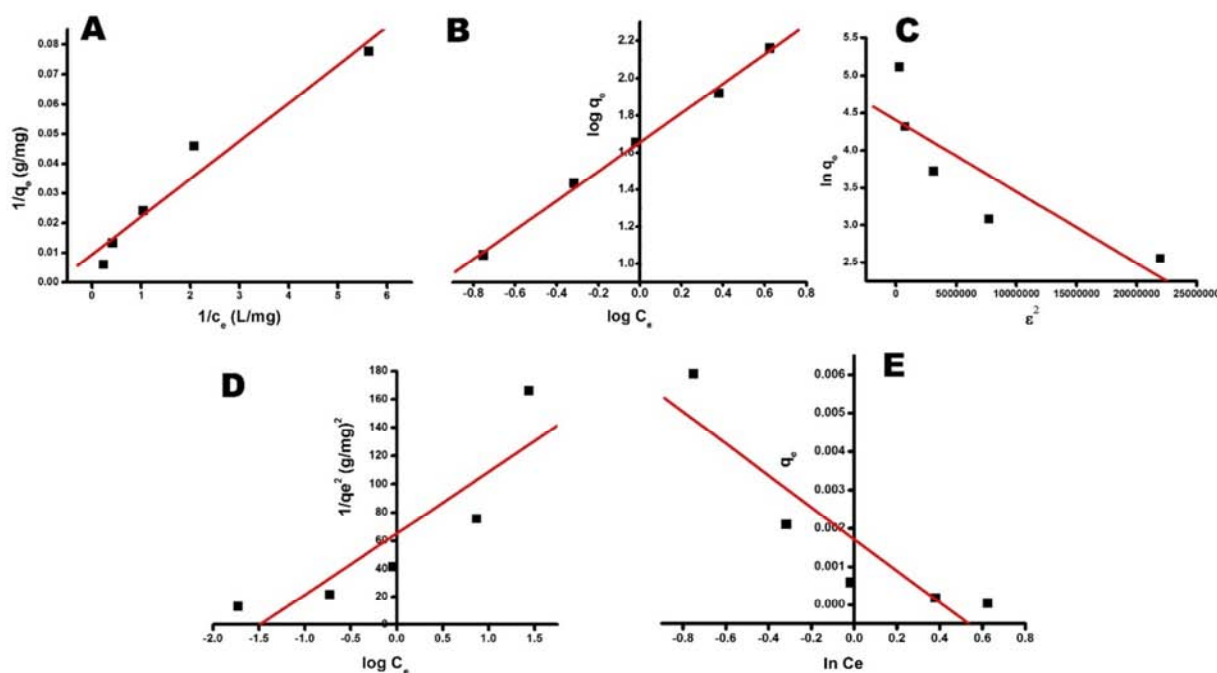


**Figure 7.** *Fitting of sorption experimental data to (A) Langmuir, (B) Freundlich, (C) Dubinin–Radushkevich (D-R), (D) Tempkin and (E) Harkins-Jura adsorption isotherms.*
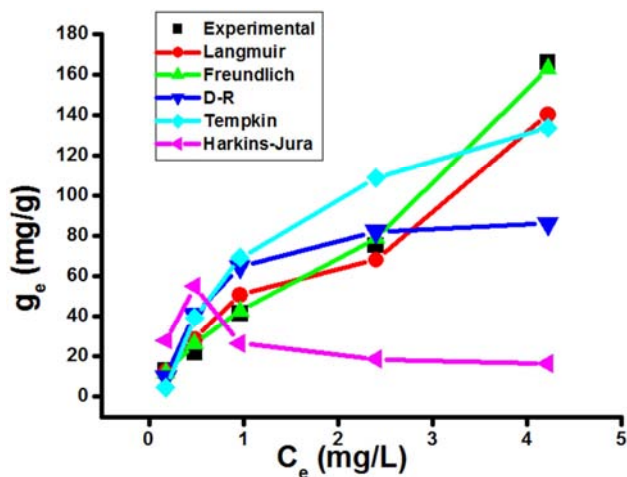
***Table 6.*** *Adsorption isotherm parameters for the adsorption of RhB onto GONS.*

| Adsorption isotherm parameters | | | | |
|---|---|---|---|---|
| **Langmuir isotherm** | **Freundlich isotherm** | **Dubinin-Radushkevich isotherm** | **Tempkin isotherm** | **Harkins-Jura isotherm** |
| $q_o = 105.26$ | $K_f = 47.36$ | $q_{DR} = 88.61$ | $b_T = 51.83$ | $A_{HJ} = -270.27$ |
| $k_a = 0.7731$ | $n = 1.24$ | $\beta = 1 \times 10^{-7}$ | $A_T = 4.36$ | $B_{HJ} = -0.4054$ |
| $r^2 = 0.952$ | $r^2 = 0.998$ | $r^2 = 0.7303$ | $r^2 = 0.780$ | $r^2 = 0.819$ |
| $R_L = 0.0415$ | | | | |

Correlation between the adsorption isotherm models and the sorption experimental data were verified using error analysis, Eqns. 3, 4 and 5. The results of the analysis are listed in Table 7. The lower the values of SD, $u$, and $\chi^2$, the better the model for the sorption processes, hence Freundlich model is the best among the models considered in this work. The calculated $q_e$ of Freundlich isotherm model fitted well to the experimental adsorption capacity ($q_e$) than other tested models, Figure 8, suggesting that the sorption processes of RhB by GONS is compatible with the heterogeneous surface law.

Comparative Adsorption parameters of Rhodamine B on various adsorbents in aqueous solution with present work are summarized in Table 8 [27, 57, 61−65]. The percentage adsorption in this work are relatively higher or comparable to previous works. It is noteworthy to mention that the process of adsorption in this work was completed within the first 5 min compared to previous works, suggesting that the nanosheets of graphene oxide is a better adsorbent. Also, the pH and adsorbent dose are within the acceptable optimum conditions required for the removal of RhB in water using GONS.



***Figure 8.*** *Comparison of the experimental and predicted isotherm models for the sorption of RhB by GONS at the optimum pH.*

***Table 7.*** *Error analysis for isotherm models for the sorption of RhB on GONS.*

| Model | Parameters | Initial concentration (mg/L) | | | | |
|---|---|---|---|---|---|---|
| | | **2.49** | **4.79** | **9.87** | **15.09** | **29.85** |
| | $SD$ | 0.478 | 0.923 | 1.380 | 1.183 | 2.265 |
| Langmuir isotherm | $\chi^2$ | 0.021 | 1.633 | 0.276 | 0.716 | 4.682 |
| | $u$ | 0.214 | 0.413 | 0.617 | 0.529 | 1.013 |
| | $SD$ | 0.192 | 0.513 | 0.775 | 0.839 | 0.777 |
| Freundlich isotherm | $\chi^2$ | 0.002 | 0.066 | 0.210 | 0.375 | 0.056 |
| | $u$ | 0.086 | 0.229 | 0.245 | 0.157 | 0.347 |
| | $SD$ | 0.693 | 1.957 | 2.167 | 1.171 | 4.001 |
| Dubinin-Radushkevich isotherm | $\chi^2$ | 0.943 | 8.958 | 0.969 | 0.574 | 74.37 |
| | $u$ | 0.309 | 0.875 | 8.510 | 0.524 | 1.789 |
| | $SD$ | 1.230 | 1.869 | 2.361 | 2.599 | 2.548 |
| Tempkin isotherm | $\chi^2$ | 16.07 | 0.108 | 1.056 | 10.447 | 133.8 |
| | $u$ | 0.581 | 0.836 | 11.231 | 1.162 | 1.139 |
| | $SD$ | 1.737 | 2.574 | 1.727 | 3.370 | 5.478 |
| Harkins-Jura isotherm | $\chi^2$ | 8.136 | 19.98 | 8.427 | 173.9 | 1389 |
| | $u$ | 0.777 | 1.151 | 0.772 | 1.507 | 2.450 |

***Table 8.*** *Comparative adsorption parameters of Rhodamine B on various adsorbents with present work.*

| Adsorbents | Optimum conditions (pH, adsorbent dose, mg, and temperature, K) | Equilibration time | Percentage adsorption (%) | Ref. |
|---|---|---|---|---|
| $Fe_3O_4$/MWCNT | pH 6.0, 3, 298 | 80 min | 98 | 61 |
| $Fe_3O_4$/HA | pH 6.0, 100, 298 | 20 min | 95 | 62 |
| EGO | pH 6.0, 11, 298 | 25 min | 50 | 27 |
| $CoFe_2O_4$ | pH 7.0, 50, 293 | 360 min | - | 57 |
| MWCNT–C | pH 7.0, 50, 293 | 360 min | - | 57 |
| $Fe_3O_4$-AC | pH 4.0, 30, 298 | 30 min | 98 | 63 |
| AC | pH 2.3, 8, 313 | 60 min | 66 | 64 |
| Mustard cake | pH 2.3, 8, 313 | 6 h | 57 | 64 |
| MWCNT | pH 7.0, 100 | 20 min | 65-90 | 65 |
| GONS | pH 6.5, 16. 7, 298 | 5 min | 92.9 | Present study |

### 3.2.5. Temperature and Thermodynamic Studies of Adsorption

Effect of temperature on the removal of RhB by GONS was investigated by agitating known concentrations of GONS and RhB at varying reaction temperatures of 298, 308, 318 and 328 K. The obtained results are presented in Table 9. The amount of RhB adsorbed increases with temperature, Figure 9A, suggesting that adsorption process is favoured at higher temperatures. The pore sites on the adsorbent may have increased in volume at elevated temperature resulting in the amount of RhB adsorbed. Enhanced adsorption rate of RhB at higher temperatures could be attributed to the increased kinetic energy of the adsorbate to the available sorption sites on GONS surface. Increase in the pore volumes of the adsorbents at higher temperature has been reported before [35, 52]. Thus, the process of adsorption is endothermic in nature.

**Table 9.** *Effect of temperature on adsorption of RhB onto GONS. Conditions: sorbent mass 16.67 g in 25 mL; sorbate concentration ≈30 mg/L; sorbate volume, 100 mL; pH 6.5: agitation speed 120 rpm.*

| Temperature, K | Initial conc. (mg/L) | Final conc. (mg/L) | Amount adsorbed (mg/L) | Percentage adsorbed (%) |
|---|---|---|---|---|
| 298 | 29.85 | 0.702 | 25.64 | 85.88 |
| 308 | 29.85 | 0.690 | 25.71 | 86.12 |
| 318 | 29.85 | 0.631 | 26.07 | 87.32 |
| 328 | 29.85 | 0.572 | 26.43 | 88.52 |

Thermodynamic studies were investigated on the adsorption of RhB onto GONS using parameters such as standard Gibbs energy change (ΔG°), enthalpy change (ΔH°), and entropy change (ΔS°). These parameters provide further details on the spontaneity, feasibility, and sorbate-sorbent interactions during adsorption process. Relationship between ΔG° and T is shown in Eqn. 8 [36]:

$$\Delta G^o = -RT \ln K_d \qquad (8)$$

where T is the temperature, R is the gas constant, and $K_d$, calculated as $q_e/C_e$, is the distribution coefficient. van't Hoff equation shows that $K_d$ is related to ΔH° and ΔS° in Eqn. 9 [59]:

$$\ln K_d = \frac{\Delta S^o}{R} - \frac{\Delta H^o}{RT} \qquad (9)$$

The magnitudes of ΔH° and ΔS° in Eqn. 9, were respectively calculated from the slope and intercept of van't Hoff plots of $\ln K_d$ against $1/T$, Figure 9B. The results of the calculated thermodynamic parameters for the adsorption studies are summarised in Table 10. The negative vales of ΔG° increased from −7.45 to −9.02 $kJ/mol$ as temperature increased from 298 to 328 $K$, suggesting improved feasibility and spontaneity of the RhB-GONS system at elevated temperature. The positive value of ΔS° shows that the process of adsorption of RhB onto GONS was enhanced due to increase in the degree of disorderliness at the sorbate-sorbent interface. At higher temperature, degree of disorderliness increased the adsorbate-adsorbent interactions rather than adsorbate-solvent interaction [57, 66]. Positive value of heat of adsorption, ΔH°, indicates that the process of adsorption was endothermic in nature, hence RhB uptake by GONS in aqueous solution is favored at higher temperature. This is in agreement with the results listed in Table 9 above. The value of ΔH° indicates the mechanism of adsorption to be either physisorption when ΔH° is between 2.1 to 20.9 kJ mol$^{-1}$, or chemisorption when ΔH° is between 80 to 200 kJ mol$^{-1}$[18, 67]. From Table 10, calculated value of ΔH° lies between 2.1 to 20.9 kJ mol$^{-1}$, suggesting that the mechanism of interaction between RhB and GONS in water is governed by physisorption.
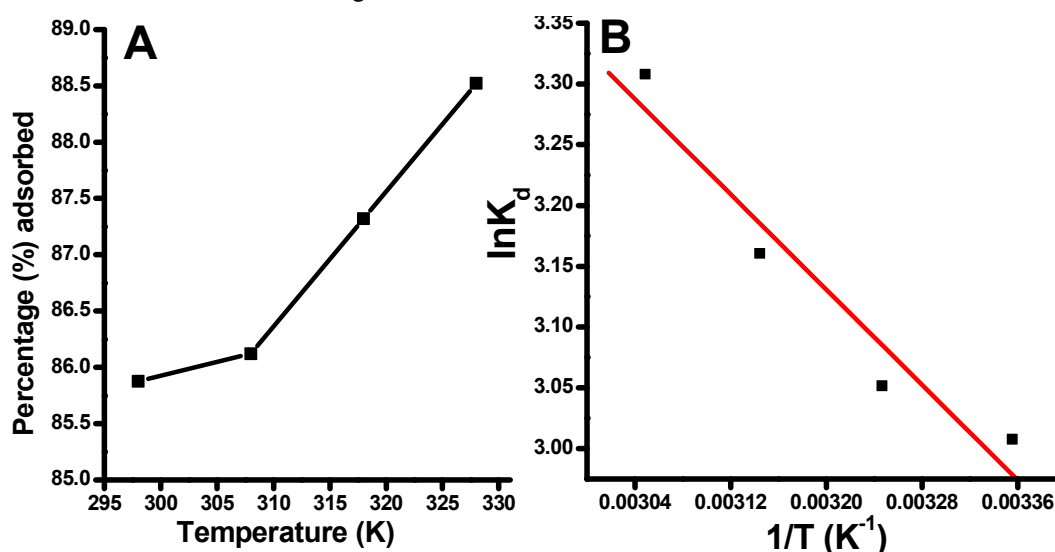


**Figure 9.** *(A) Variation of Temperature (T) against percentage, %, adsorbed, and (B) Van't Hoff plots of $\ln K_d$ vs $1/T$ for adsorption of RhB onto GONS.*

**Table 10.** *Thermodynamic parameters for the adsorption of RhB onto GONS.*

| Temperature, K | $\Delta G°$, (kJ/mol) | $\Delta H°$, (kJ/mol) | $\Delta S°$, $(JK^{-1}mol^{-1})$ |
|---|---|---|---|
| 298 | $-7.45 \pm 0.12$ | $8.15 \pm 0.12$ | $52.10 \pm 0.08$ |
| 308 | $-7.81 \pm 0.31$ | – | – |
| 318 | $-8.36 \pm 0.09$ | – | – |
| 328 | $-9.02 \pm 0.06$ | – | – |

### 3.3. Adsorption Mechanism (FTIR)

Mechanism of adsorption between the adsorbate and adsorbent was confirmed by comparing the FTIR spectra of GO-RhB system before and after adsorption studies, Figure 10. Characteristics absorption bands at 3253-3585 cm⁻¹, and small but clearly visible peak at 1699 cm⁻¹, are respectively attributed to the presence of alcoholic hydroxyl and carbonyl groups on GO, Figure 10. Absorption band at 1604 cm⁻¹ in the IR spectrum of GO is attributed to the aromatic C=C groups. FTIR investigations of RhB confirmed the presence of ($= N^+$) immonium ion at 1595 cm⁻¹, and heterocycle skeleton of RhB molecule at 1342 and 1178 cm⁻¹ [68], Figure 10. The vibration signals at 1342, 1178 and 1073 cm⁻¹, attributed to heterocycle skeleton of RhB molecule, are consistent in the spectra of RhB as well as the GO-RhB. The intense $- CO_2$ bands in GO, RhB and GO-RhB, are due to irreversible adsorption of $- CO_2$ on the surface of the GO and RhB. The characteristics peak around 1699 cm⁻¹ in GO (Figure 10) disappeared in the IR spectrum of GO-RhB system, Figure 10, suggesting that the mechanism of adsorption was due to possible electrostatic interactions between protonated carbonyl ($-COO^-$) groups on GO nanosheets, and positively charged immonium ($= N^+$) ions of RhB molecules in water, Figure 11. Adsorption mechanisms due to electrostatic interaction, intermolecular hydrogen bonding and π-π interaction have been reported as major mechanisms for graphene based adsorbents for organic dyes removal [69-71]. Adsorption mechanism due to intermolecular hydrogen bonding between RhB and GONS cannot be ruled out since multilayer surface coverage dominates the sorption process of RhB-GONS system [69], as observed from the results of kinetic studies above. Also, adsorption process can arise due to π–π stacking interaction of the aromatic ring of rhodamine B dye with the nanosheets of graphene oxides.
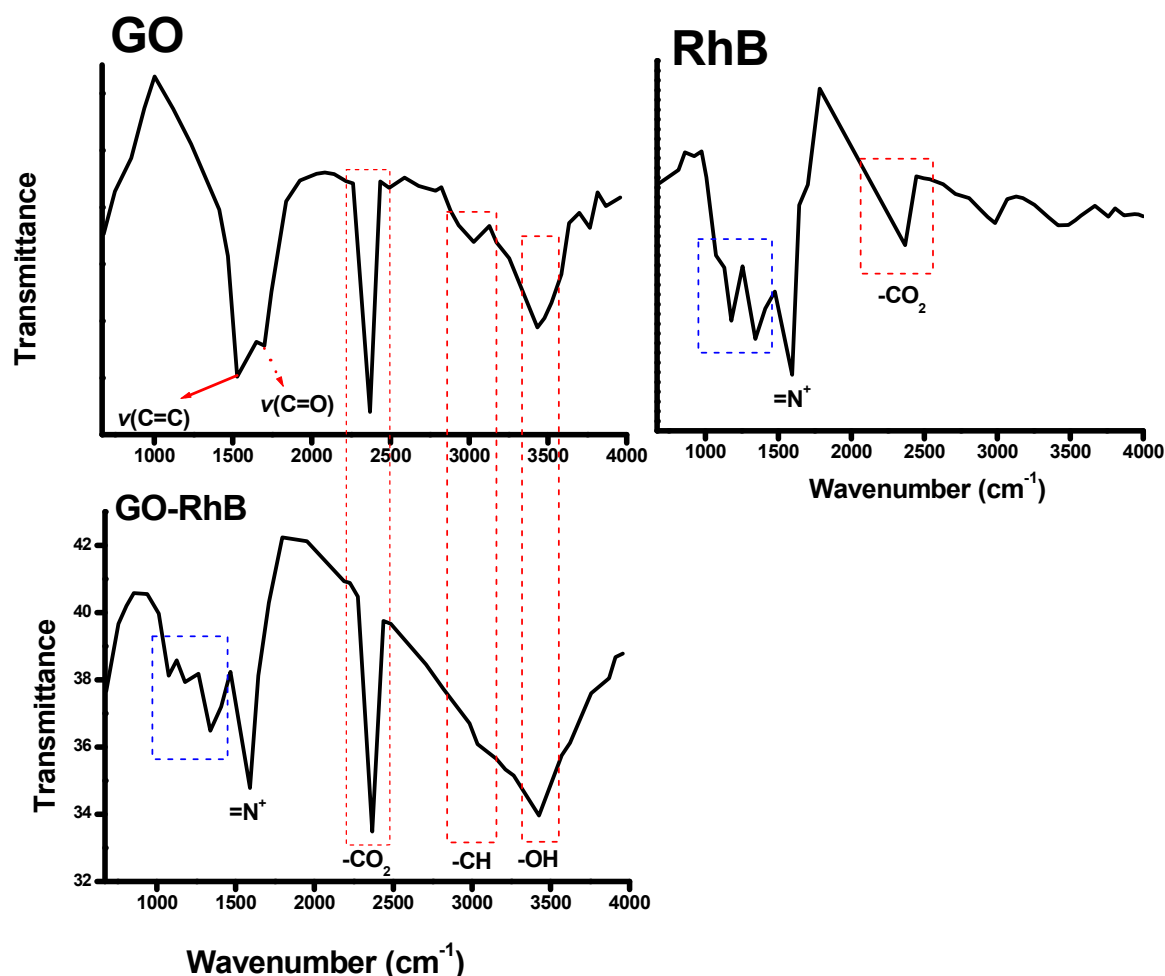


**Figure 10.** *FTIR spectra of graphene oxide (GO), Rhodamine B (RhB), and Rhodamine B loaded graphene oxide (GO-RhB).*
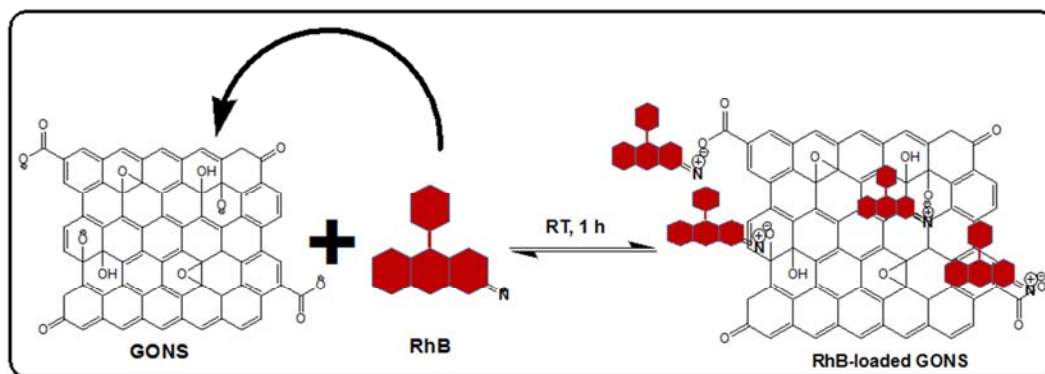
*Figure 11. Schematic illustration of the adsorption and desorption of RhB onto GONS.*

### 3.4. Desorption Studies

Ease of regeneration of spent adsorbent was investigated to determine the reusability of the adsorbent after adsorption experiments, and to further understand the mechanism of adsorption between RhB and GONS. Desorbing eluents such as water, methanol and methanol/acetic acid (9:1), were used to desorb RhB from the surface of the GONS. Efficiency of the desorbing eluents was calculated by comparing the amount of RhB desorbed from GONS to the amount of RhB in RhB-loaded adsorbent, using Eqn 10 [72].

$$\text{Desorption efficiency (\%)} = \frac{q_{de}}{q_{ad}} \times 100 \qquad (10)$$

where $q_{de}$ is the quantity of RhB desorbed by desorbing eluents and $q_{ad}$ is the amount of RhB adsorbed in RhB-loaded adsorbent.

Desorption efficiencies estimated for methanol/acetic acid (9:1), methanol and water are 94.21%, 71.36% and 45.52%, respectively. The higher the desorption efficiency, the better the solvent as desorbing eluent to regenerate both the spent adsorbent and adsorbate for further use, hence methanol solution of acetic acid (10%) has better desorptive property compared to methanol and water. Zhou et al., [37] demonstrated that 75% of MB could be desorbed from the surface of $Fe_3O_4$/GO using 5% acetic acid in methanol solution. Also, up to 82% of RhB was reportedly removed from the surface of DNc using only acetic acid as desorbing eluent [72]. Herein, $\approx$ 94% desorption efficiency of RhB from GO was achieved using 10% of acetic acid in methanol solution. The ease at which RhB was eluted from RhB-loaded GO using methanol/acetic acid (9: 1), methanol and water shows that the adsorption mechanism is best described by physisorption.

## 4. Conclusion

Investigations into kinetics and thermodynamic studies of Rhodamine B removal in aqueous solution onto graphene oxides have been carried out in this work. The prepared graphene oxides were characterized using techniques such as UV, TEM, FTIR, EDX and XRD. Removal of RhB dye in simulated wastewater onto GONS was carried out under different optimized experimental conditions, including change in pH, initial concentrations, adsorbent dosage, temperature, and contact time. At temperature of 298K and pH 6.5, 92.87% of RhB was found to have been removed onto 16.67mg of GONS at optimized contact time of 60 min, and concentration of 2.5 mg/L. Experimental data tested against results of the kinetics and adsorption isotherm models showed that the removal of RhB were best fitted to pseudo-second order and Freundlich models, respectively. Desorption studies were carried out on the spent GONS to determine its reusability for further adsorption experiments. Desorbing eluents such as water, methanol and methanol/acetic acid (9:1), were used to remove adhered RhB from the surface of the GONS. Methanol/acetic acid solution was observed to remove ~94% of adsorbed RhB from GO surface compared to water (71.36%) and methanol (45.52%). The ease at which RhB was eluted from RhB-loaded GO using Methanol/acetic acid solution shows that the adsorption mechanism could be best described by physisorption.

## Conflict of Interests

The authors declare that there is no conflict of interests regarding the publication of this paper.

## References

[1] M. Beija, C. A. M. Afonso, J. M. G. Martinho, Synthesis and applications of Rhodamine derivatives as fluorescent probes, Chem. Soc. Rev. 38 (2009) 2410–2433.

[2] L. Li, X. Z. Tian, G. Z. Zou, Z. K. Shi, X. L. Zhang, W. R. Jin, Quantitative counting of Single fluorescent molecules by combined electrochemical adsorption accumulation and total internal reflection fluorescence microscopy, Anal. Chem. (2008) 3999–4006.

[3]   M. Bossi, J. Folling, V. N. Belov, V. P. Boyarskiy, R. Medda, A. Egner, C. Eggeling, A. Schonle, S. W. Hell, Multicolor far-field fluorescence nanoscopy through isolated detection of distinct molecular species, Nano Lett. 8 (2008) 2463–2468.

[4]   K. H. Drexhage, Fluorescence efficiency of laser dyes, J. Res. Natl. Bur. Stand. 80A (1976) 421–428.

[5]   K. H. Drexhage, Solvent dependence of the fluorescence lifetimes of xanthene dyes, Laser Focus 9 (1973) 35–39.

[6]   J. P. S. Farinha, M. T. Charreyre, J. M. G. Martinho, M. A. Winnik and C. Pichot, Picosecond fluorescence studies of the surface morphology of charged polystyrene latex particles, Langmuir, 17 (2001) 2617–2623.

[7]   T. Fonseca, P. J. M. G. Martinho and J. P. S. Farinha, Preparation and surface characterization of polymer nanoparticles designed for incorporation into hybrid materials, Langmuir, 23 (2007) 5727–5734.

[8]   J. Anandkumar, B. Mandal, Adsorption of chromium (VI) and rhodamine B by surface modified tannery waste: kinetic, mechanistic and thermodynamic studies, J. Hazard. Mater. 186 (2011) 1088-1096.

[9]   S. K. Das, P. Ghosh, I. Ghosh, A. K. Guha, Adsorption of rhodamine B on *Rhizopus oryzae*: Role of functional groups and cell wall components, J Colloids Surf. B 65 (2008) 30–34.

[10]  M. Das, K. G. Bhattacharyya, Oxidation of rhodamine B in aqueous medium in ambient conditions with raw and acid-activated $MnO_2$, NiO, ZnO as catalysts, J Mol. Catal. A Chem. 391 (2014) 121–129.

[11]  S. Nadupalli, N. Koorbanally, S. B. Jonnalagadda, Chlorine dioxide-facilitated oxidation of the azo dye amaranth, J. Phys. Chem. A 115 (2011) 11682–11688.

[12]  B. Pare, B. B. Sarwan, S. Jonnalagadda, Photocatalytic mineralization study of malachite green on the surface of Mn-doped BiOCl activated by visible light under ambient condition, Appl. Surf. Sci. 258 (2011) 247–253.

[13]  A. L. Ahmad, W. A. Harris, Syafiie, O. B. Seng, Removal of dye from wastewater of textile industry using membrane technology, Jurnal Teknologi 36 (2002) 31–44.

[14]  L. Wojnarovits, E. Takacs, Irradiation treatment of azo dye containing wastewater: An overview, Radiat. Phys. Chem. 77 (2008) 225–244.

[15]  P. Dachipally, S. B. Jonnalagadda, Kinetics of ozone-initiated oxidation of textile dye, Amaranth in aqueous systems, J. Environ. Sci. Health, Part A 46 (2011) 887–897.

[16]  Y. Yan, M. Zhang, K. Gong, L. Su, Z. Guo and L. Mao, Adsorption of Methylene Blue Dye onto Carbon Nanotubes: A Route to an Electrochemically Functional Nanostructure and Its Layer-by-Layer Assembled Nanocomposite, Chem. Mater. 17 (2005) 3457–3462.

[17]  S. B. Jonnalagadda, S. Nadupalli, Effluent treatment using electrochemically bleached seawater—oxidative degradation of pollutants, Talanta 64 (2004) 18–22.

[18]  I. A. A. Hamza, B. S. Martincigh, J. C. Ngila, V. O. Nyamori, Adsorption studies of aqueous Pb (II) onto a sugarcane bagasse/multi-walled carbon nanotube composite, Phys. Chem. Earth 66 (2013) 157–166.

[19]  S. C. Tan, P. Shi, R. J. Su, M. C. Zhu, Removal of methylene blue from aqueous solution by powdered expanded graphite: adsorption isotherms and thermodynamics, Adv. Mat. Res. 424-425 (2012) 1313-1317.

[20]  M. Caragiu, S. Finberg, Alkali metal adsorption on graphite: A review, J. Phys. Condens. Matter 17 (2005) R995-R1024.

[21]  M. Zhao, P. Liu, Adsorption of methylene blue from aqueous solutions by modified expanded graphite powder, Desalination 249 (2009) 331-336.

[22]  K. M. Hock, R. E. Palmer, Temperature dependent behaviour in the adsorption of submonolayer potassium on graphite, Surf. Sci. 284 (1993) 349-360.

[23]  Y. Si, E. T. Samulski, Synthesis of water soluble graphene, Nano Lett. 8 (2008) 1679-1682.

[24]  F. Liu, S. Chung, G. Oh, T. Seok, Three-dimensional graphene oxide nanostructure for fast and efficient water-soluble dye removal, ACS Appl. Mater. Interfaces 4(2) (2012) 922-927.

[25]  P. Bradder, S. K. Ling, S. Wang, S. Liu, Dye adsorption on layered graphite Oxide, J. Chem. Eng. Data 56 (2011) 138−141.

[26]  P. Sharma, M. R. Das, Removal of a Cationic dye from aqueous solution using graphene oxide nanosheets: investigation of adsorption parameters, J. Chem. Eng. Data 58 (2102) 151-158.

[27]  G. K. Ramesha, A. Vijaya Kumara, H. B. Muralidhara, S. Sampath, Graphene and graphene oxide as effective adsorbents toward anionic and cationic dyes, J. Colloid Interface Sci. 361 (2011) 270–277.

[28]  S. Mukhtar, M. Liu, J. Han, W. Gao, Removal of rhodamine B from aqueous solutions using vanadium pentoxide/titanium butyl oxide hybrid xerogels, Chin. Phys. B 26 (2017) 058202.

[29]  G. Sharifzade, A. Asghari, M. Rajabi, Highly effective adsorption of xanthene dyes (Rhodamine B and erythrosine B) from aqueous solutions onto lemon citrus peel active carbon: characterization, resolving analysis, optimization and mechanistic studies, RSC Adv., 7 (2017) 5362–5371.

[30]  G. Vijayakumar, C. K. Yoo, K. G. P. Elango, M. Dharmendirakumar, Adsorption characteristics of rhodamine B from aqueous solution onto baryte, Clean 38 (2010) 202–209.

[31]  M. Wang, J. Fu, Y. Zhang, Z. Chen, M. Wang, J. Zhu, W. Cui, J. Zhang, Q. Xua, Removal of Rhodamine B, a cationic dye from aqueous solution using poly (cyclotriphosphazene-co-4,4'-sulfonydiphenol) nanotubes, J. Macromol. Sci., Pure Appl. Chem. 52 (2015) 105–113.

[32]  J. Ma, D. Ping, X. Dong, Recent developments of graphene oxide-based membranes: A review, Membranes (Basel). 7 (2017) 52-80.

[33]  W. S. Hummers, R. E. Offeman, Preparation of graphitic oxide, J. Am. Chem. Soc. 80 (1958) 1339–1339.

[34]  Z. Bo, X. Shuai, S. Mao, H. Yang, J. Qian, J. Chen, J. Yan, K. Cen, Green preparation of reduced graphene oxide for sensing and energy storage applications, Sci. Rep. 4 (2014) 4684-4691.

[35]  T. A. Khan, M. Nazir and E. A. Khan, Adsorptive removal of Rhodamine B from textile wastewater using water chestnut (*Trapa natans L.*) peel: adsorption dynamics and kinetics studies, Toxicol. Environ. Chem. 95 (2013) 919–931.

[36] L. S. Balistrieri and J. W. Murray, The surface chemistry of goethite (alpha FeOOH) in major ion seawater, Am. J. Sci. 281 (1981) 788–806.

[37] C. Zhou, W. Zhang, H. Wang, H. Li, J. Zhou, S. Wang, J. Liu, J. Luo, B. Zou, J. Zhou, Preparation of $Fe_3O_4$-embedded graphene oxide for removal of methylene blue, Arab. J. Sci. Eng. 39(9) (2014) 6679-6685.

[38] A. I. Vogel, Text Book of Practical Organic Chemistry, Longman, London, UK, 1970.

[39] I. Langmuir, The adsorption of gases on plane surfaces of glass, mica and platinum, J. Am. Chem. Soc., 40 (1918) 1361–1402.

[40] H. Freundlich, Over the adsorption in solution, Z. Phys. Chem., 57 (1906) 385–470.

[41] M. M. Dubinin, L. V. Radushkevich, The equation of the characteristic curve of the activated charcoal, Proc. Natl. Acad. Sci. USSR Phys. Chem. Sect. 55 (1947) 331–337.

[42] M. I. Temkin, V. Pyzhev, Kinetic of ammonia synthesis on promoted iron catalyst, Acta Phys. Chim., 12 (1940) 327–356.

[43] A. Kausar, H. N. Bhatti, G. MacKinnon, Equilibrium, kinetic and thermodynamic studies on the removal of U (VI) by low cost agricultural waste, Colloids Surf B Biointerfaces 111 (2013) 124-133.

[44] Y. S. Ho, Water Res., Comment on "cadmium removal from aqueous solutions by chitin: kinetic and equilibrium studies", 38 (2004) 2962–2964.

[45] Y.-S. Ho, Water Res. Removal of copper ions from aqueous solution of tree fern, 37 (2003) 2323–2330.

[46] J. Lin, L. Wang, Comparison between linear and non-linear forms of pseudo-first-order and pseudo-second-order adsorption kinetic models for the removal of methylene blue by activated carbon, Front. Environ. Sci. Eng. 3 (2009) 320–324.

[47] Y. S. Ho, G. McKay, Kinetic models for the sorption of dye from aqueous solution by wood, Process Saf. Environ. Prot., 76 (1998) 183–191.

[48] J. Zeldowitsch, "About the mechanism of catalytic oxidation of CO to $MnO_2$", Acta Physicochimica URSS 1 (1934) 449–464.

[49] S. H. Chien, W. R. Clayton, Application of Elovich equation to the kinetics of phosphate release and sorption in soils, Soil Sci. Soc. Am. J., 44 (1980) 265–268.

[50] S. Verma, H. P. Mungse, N. Kumar, S. Choudhary, S. L. Jain, B. Sain, O. P. Khatri, Graphene oxide: an efficient and reusable carbocatalyst for aza-Michael addition of amines to activated alkenes, Chem. Commun. 47 (2011) 12673-12675.

[51] M. Shi-Jia, S. Yu-Chang, X. Li-Hua, L. Si-Dong, H. Te, T. Hong-Bo, X-ray diffraction pattern of graphite oxide, Chinese Phys. Lett. 30(9) (2013) 096101-096103.

[52] T. A. Khan, S. Dahiya, I. Ali, Use of kaolinite as adsorbent: equilibrium, dynamics and thermodynamic studies on the adsorption of Rhodamine B from aqueous solution, Appl. Clay Sci. 69 (2012) 58–66.

[53] H. M. H. Gad, A. A. El-Sayed, Activated carbon from agricultural by-products for the removal of Rhodamine B from aqueous solution, J. Hazard. Mater. 168 (2009) 1070-1081.

[54] E. Akar, A. Altinisik, Y. Seki, Using of activated carbon produced from spent tea leaves for the removal of malachite green from aqueous solution, Ecol. Eng. 52 (2013) 19-27.

[55] M. Ozacar, I. A. Sengil, Adsorption of metal complex dyes from aqueous solutions by pine sawdust, Bioresour. Technol. 96 (2005) 791–795.

[56] A. Shukla, Y. H. Zheng, P. Dubey, J. L. Margrare, S. S. Shukla, The role of sawdust in the removal of unwanted materials from water, J. Hazard. Mater. 95 (2002) 137–152.

[57] O. A. Oyetade, V. O. Nyamori, B. S. Martincigh, S. B. Jonnalagadda, Effectiveness of carbon nanotube–cobalt ferrite nanocomposites for the adsorption of rhodamine B from aqueous solutions, RSC Adv., 5 (2015) 22724–22739.

[58] Y. S. Ho, A. E. Ofomaja, Pseudo-second-order model for lead ion sorption from aqueous solutions onto palm kernel fiber, J. Hazard. Mater. 129 (2006) 137–142.

[59] L. Ai, L. M. Li, L. Li, Adsorption of methylene blue from aqueous solution with activated carbon/cobalt ferrite/Alginate composite beads: kinetics, isotherms, and thermodynamics, J. Chem. Eng. Data 56 (2011) 3475−3483.

[60] T. W. Weber, R. K. Chakravorti, Pore and solid diffusion models for fixed-bed adsorbers, AIChE J. 20 (1974) 228−238.

[61] K. Kerkez and S. S. Bayazit, Magnetite decorated multi walled carbon nanotubes for removal of toxic dyes from aqueous solutions, J. Nanopart. Res. 16 (2014) 2431–2441.

[62] L. Peng, P. Qina, M. Lei, Q. Zeng, H. Song, J. Yang, J. Shao, B. Liao and J. Gua, Modifying $Fe_3O_4$ nanoparticles with humic acid for removal of Rhodamine B in water, J. Hazard. Mater. 209-210 (2012) 193–198.

[63] T. Madrakian, A. Afkhami, H. Mahmood-Kashani, M. Ahmad, Adsorption of some cationic and anionic dyes on magnetite nanoparticles modified activated carbon from aqueous solutions: equilibrium and kinetics study, J. Iran. Chem. Soc. 10(3) (2013) 481-489.

[64] V. K. Gupta, R. Jain, M. N. Siddiqui, T. A. Saleh, S. Agarwal, S. Malati and D. Pathak, Equilibrium and thermodynamic studies on the adsorption of the dyeJ. Chem. Eng. Data, 55 (2010) 5225–5229.

[65] S. Kumar, G. Bhanjana, K. Jangra, N. Dilbaghi and A. Umar, Utilization of carbon nanotubes for the removal of Rhodamine B dye from aqueous solutions, J. Nanosci. Nanotechnol. 14 (2014) 4331–4336.

[66] M. A. Malana, S. Ijaz, M. N. Ashiq, Removal of various dyes from aqueous media onto polymeric gels by adsorption process: their kinetics and thermodynamics, Desalination 263 (2010) 249–257.

[67] Y. Liu, Y.-J. Liu, Biosorption isotherms, kinetics and thermodynamics, Sep. Purif. Technol. 61 (2008) 229–242.

[68] O. V. Ovchinnikov, S. V. Chernykh, M. S. Smirnov, D. V. Alpatova, R. P. Vorob'eva, A. N. Latyshev, A. B. Evlev, A. N. Utekhin, A. N. Lukin, Analysis of interaction between the organic dye methylene blue and the surface of AgCl (I) microcrystals, J. Appl. Spectrosc. 74 (2007) 809−816.

[69] H. Kim, S. O. Kang, S. Park and H. S. Park, Adsorption isotherms and kinetics of cationic and anionic dyes on three-dimensional reduced graphene oxide macrostructure, J. Ind. Eng. Chem. 21 (2015) 1191-1196.

[70] X. P. Wang, Z. M. Liu, X. P. Ye, K. Hu, H. Q. Zhong, J. F. Yu, M. Jin, Z. Y. Guo, A facile one-step approach to functionalized graphene oxide-based hydrogels used as effective adsorbents toward anionic dyes, Appl. Surf. Sci. 308 (2014) 82-90.

[71] S.-T. Yang, S. Chen, Y. Chang, A. Cao, Y. Liu and H. Wang, Removal of methylene blue from aqueous solution by graphene oxide, J. Colloid Interface Sci. 359 (2011) 24-29.

[72] A. A. Inyinbor, F. A. Adekola, G. A. Olatunji, Liquid phase adsorptions of Rhodamine B dye onto raw and chitosan supported mesoporous adsorbents: isotherms and kinetics studies, Appl. Water Sci. 7 (2016) 2297-2307.